

Effect of Nb⁵⁺ doping on microwave dielectric properties of MgTa₂O₆ ceramic

Liang Shi*, Cheng Liu, Huaiwu Zhang*

School of Electronic Science and Engineering, University of Electronic Science and Technology of China, Chengdu, 610054, China

*Corresponding Author: Huaiwu Zhang: hwzhang@uestc.edu.cn,

Shi Liang: 201911022405@std.uestc.edu.cn

Abstract. As the main carrier for microwave circuits, microwave dielectric ceramics are receiving a lot of attention as the main carrier for the current 5G and pre-developed 6G communication technologies. A series of Nb⁵⁺ doped MgTa₂O₆ ceramics were synthesized by the solid-state reaction method X-ray diffraction confirmed that a single tetragonal structure can be formed when the doping amount is lower than 0.03, a heterogeneous structure of tetragonal and orthorhombic crystal structure is formed when the doping amount is lower than 0.15, and the tetragonal structure is completely transformed into orthorhombic structure when the doping exceeds 0.15. SEM results also show the transformation process of the grains of tetragonal structure to orthorhombic structure. The optimum microwave dielectric properties were obtained for 9% Nb⁵⁺ doped samples: $\epsilon_r = 24$, $Q \times f = 71,000$ GHz (at 8.9 GHz), TCF = 15 ppm/°C.

Keywords: MgTa₂O₆, ceramic, microwave dielectric properties.

1. Introduction

With the continuous development and innovation of wireless communication technology, such as 5G, Internet of Things, and the pre-research of 6G communication technology, higher requirements are put forward for microwave circuits: high frequency, low loss, and good stability. As the main raw material for microwave circuits, the intrinsic properties of microwave dielectric ceramics directly determine the viability of microwave circuits. A suitable ceramic raw material should have good microwave dielectric properties, including high operating frequency, good dielectric response (ϵ_r), low dielectric loss (high $Q \times f$ value), and good thermal stability (TCF) [1]. Currently, researchers are sparing no efforts to explore new and modified microwave dielectric ceramic substrates to adapt to the high frequency and high power requirements of modern millimeter wave communication technology. Up to now, a series of novel composite dielectric ceramics with excellent microwave dielectric properties have been discovered, such as Ln₂Zr₃(MoO₄)₉ (Ln=Ce, La, Eu) [2-4], Eu₂TiO₅ [5], Eu₃NbO₇ [6], EuNbO₄ [7].

Considering that Nb⁵⁺ and Ta⁵⁺ have very similar physicochemical properties, especially electronegativity ($X_{\text{Nb}}=1.6$, $X_{\text{Ta}}=1.5$) and ionic radius ($R_{\text{Nb}}=R_{\text{Ta}}=0.64\text{\AA}$), it is plausible that Nb⁵⁺ and Ta⁵⁺ can be partially or even fully substituted in the compound, which has been confirmed in numerous reports [8-10]. In this work, we synthesized partial Nb⁵⁺ doped MgTa₂O₆ ceramics by the traditional solid-state reaction method. Meanwhile, we investigated the phase composition by XRD, and morphology of the doped ceramics to accurately describe the dependence between microwave dielectric properties and the phase structure of the compound.

2. Experiment

High purity (purity>99.9%) starting materials powder of MgO, Nb₂O₅ and Ta₂O₅ were prepared in molar ratio according to the formula Mg(Ta_{1-x}Nb_x)₂O₆ (x=0.03-0.15). Then the oxide powders were mixed with deionized water into the nylon tank and ball mill it for 10 h through the planetary ball mill. Then the mixed slurry was dried and ground into fine powder, and the fine powder is calcined through 1100 °C for 4 h to form the phase. Subsequently, the calcined powder was mixed

with 13 wt.% of polyvinyl alcohol (PVA) binder and ground into small particles that fit through a 60 mesh sample sieve. The particles were put into a mold and pressed into a cylinder of 12 mm diameter and 6 mm thickness under 10 MPa. Finally, the cylinders were sintered at 1300-1400 °C for 6 h in air. By recording the resonant frequencies at different temperatures, the TCF value could be calculated:

$$TCF, \tau_f = \frac{f_T - f_{T_0}}{(T - T_0) \times f_{T_0}} \times 10^6 \text{ ppm}/^\circ\text{C} \quad (1)$$

T and T₀ is the high temperature and the room temperature, and similarly, f_T and f_{T₀} indicate the resonant frequencies at temperature T and T₀.

3. Results and discussion

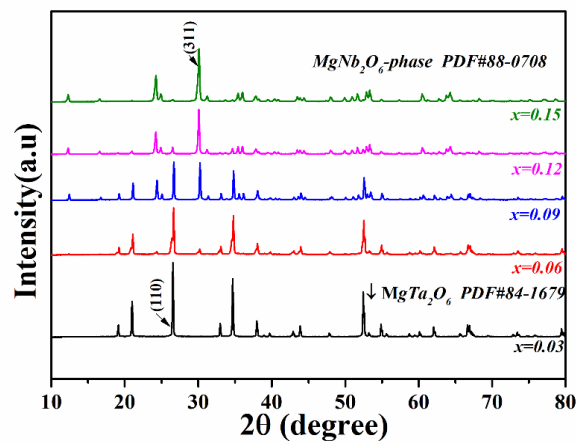


Figure 1. The XRD of Mg(Ta_{1-x}Nb_x)₂O₆ ceramics

The X-ray diffraction patterns of the samples sintered at different temperatures are shown in Figure 1. It shows that at a doping amount x of 0.03, the compound has only a tetragonal crystal structure of MgTa₂O₆, indicating that Nb⁵⁺ enters the crystal and occupies the Ta site at this time. However, with the increase of doping amount, the XRD pattern shows the superposition of diffraction peaks of tetragonal structure and orthogonal structure, which means that the excess Nb does not enter the MgTa₂O₆ crystal when the doping amount is higher than 0.06, but reacts with Mg to form the orthogonal structure of MgNb₂O₆ structure. At higher doping amounts of 0.15, the tetragonal structure can hardly be identified in the XRD patterns anymore, implying that only the orthorhombic structure exists in the compound at this time.

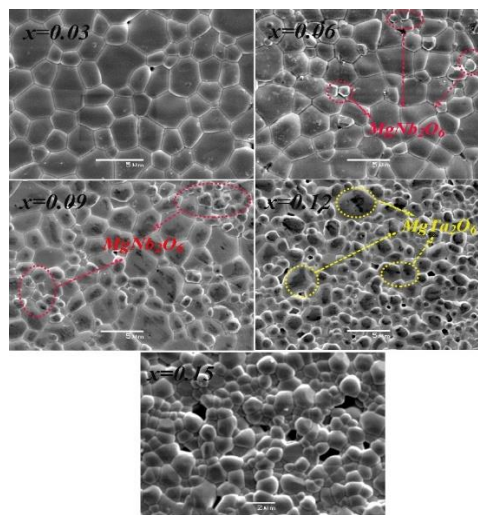


Figure 2. The SEM of Nb-doped MgTa₂O₆ ceramics

Figure 2. shows the micromorphology of the doped ceramics with different x value. At the doping amount of 0.03, flat and uniform grain distribution and clear grain boundaries were observed, but at the doping amount of 0.06, a few small grains with rounded grain boundaries appeared, and these small grains were orthogonal structure of $MgNb_2O_6$; when the doping amount was further increased to 0.09 and 0.12, the number of small grains increased significantly and gradually increased to the dominant grains. When the doping amount reaches 0.15, it is almost impossible to identify the $MgTa_2O_6$ grains, at which the grains complete the transformation from large to small, implying again the transformation of the compound from a tetragonal mechanism to an orthorhombic structure.

The variation curve of dielectric constant with sintering temperature and doping amount is shown in Figure 3. At temperatures below 1375 °C, as the sintering temperature increasing, the grain size and grain boundaries grow continuously, resulting in tighter grain arrangement and fewer pores, which is the main reason for the increasing of dielectric constant during this period[11]. After further increasing to 1375 °C and 1400 °C, the dielectric constant reached a saturation value. With the increase of doping amount, it is obvious that the dielectric constant decreases from 28 to 16. At the stage when the doping amount is lower than 0.15, there are two phases of $MgTa_2O_6$ and $MgNb_2O_6$ in the compound at this time, and since the dielectric constant of $MgNb_2O_6$ is only 20, all with the increase of Nb doping, the content of $MgNb_2O_6$ phase increases, which leads to the gradual decrease of the dielectric constant.

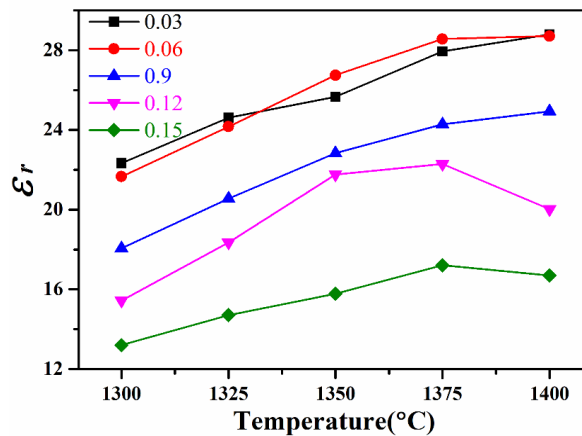


Figure 3. the variation of dielectric constant with sintering temperature and doping amount of Nb-doped $MgTa_2O_6$ ceramics

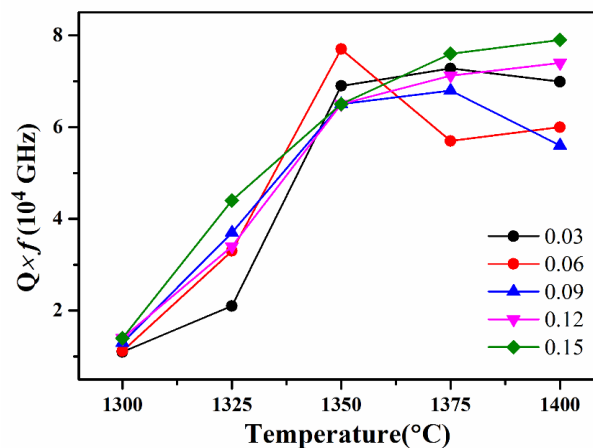


Figure 4. the variation of $Q \times f$ values with sintering temperature and doping amount of Nb-doped $MgTa_2O_6$ ceramics

The variation of $Q \times f$ values with sintering temperature are shown in figure 4. The curve of $Q \times f$ values with sintering temperature is similar to the variation of dielectric constant with temperature, both increasing first and then maintaining, due to the densification sintering process. In general, the

phase composition is an important factor affecting microwave dielectric properties [12, 13], but in this experiment, the saturation $Q \times f$ value is kept near 70,000 GHz regardless of the change in doping, this is mainly due to the $Q \times f$ values of MgTa_2O_6 and MgNb_2O_6 ceramics between 60,000 GHz and 90,000 GHz, resulting in the $Q \times f$ of their two-phase composite ceramics also fluctuate between these two values.

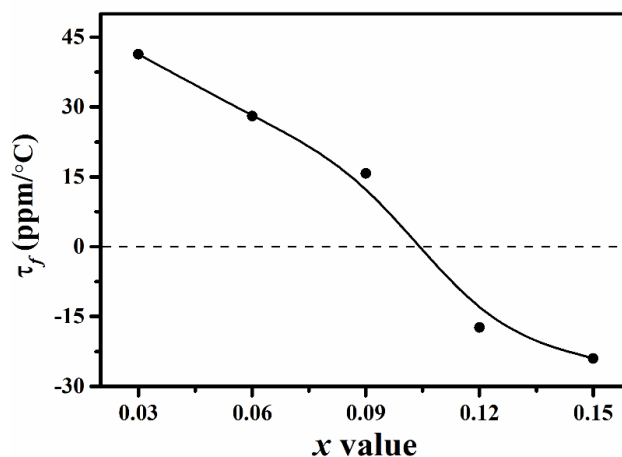


Figure 5. the variation of TCF values with doping amount of Nb-doped MgTa_2O_6 ceramics

The temperature parameter of the resonant frequency of the ceramic is an important application parameter to evaluate the operational stability of the ceramic in the environment. In order to meet the high frequency microwave circuit applications, the TCF value should be as close as possible to 0. In this experiment with the introduction of Nb, the MgNb_2O_6 phase increases accordingly, making the TCF value decrease from 40 to -20 ppm/°C for MgTa_2O_6 . This shift is mainly caused by the TCF value of -70 ppm/°C for MgNb_2O_6 .

4. Conclusion

In this study, Nb^{5+} doped $\text{Mg}(\text{Ta}_{1-x}\text{Nb}_x)_2\text{O}_6$ ($x=0.03-0.15$) ceramics are synthesized by the solid-state reaction method. Experimental results show that tetragonal structure started to transform into orthorhombic structure when doping over 0.03, and completely transformed into orthorhombic structure when the doping exceeds 0.15. The microstructure also shows the process of grain hybridization. The optimum microwave dielectric properties are obtained for 9% Nb^{5+} doped samples: $\epsilon_r = 24$, $Q \times f = 71,000$ GHz (at 8.9 GHz), $\tau_f = 15$ ppm/°C.

Acknowledgments

This work was supported by National Key Scientific Instrument and Equipment Development Project (No.51827802), and National Natural Science Foundation of China (No.51902042).

References

- [1] I.M. Reaney, D. Iddles, Microwave Dielectric Ceramics for Resonators and Filters in Mobile, *J. Am. Ceram. Soc.*, 89 (2006) 2063-2072.
- [2] H. Yang, S. Zhang, H. Yang, Y. Yuan, E. Li, $\text{Gd}_2\text{Zr}_3(\text{MoO}_4)_9$ microwave dielectric ceramics with trigonal structure for LTCC application, *Journal of the American Ceramic Society*, (2019).
- [3] B.J. Tao, C.F. Xing, W.F. Wang, H.T. Wu, Y.Y. Zhou, A novel $\text{Ce}_2\text{Zr}_3(\text{MoO}_4)_9$ microwave dielectric ceramic with ultra-low firing temperature, *Ceram. Int.*, (2019).
- [4] W. Liu, R. Zuo, A novel low-temperature firable $\text{La}_2\text{Zr}_3(\text{MoO}_4)_9$ microwave dielectric ceramic, *Journal of the European Ceramic Society*, 38 (2018) 339-342.

- [5] Z. Jinjie, Y. Yaokang, W. Haitao, Y. Zhou, Z. Zhang, Structure, infrared spectra and microwave dielectric properties of the novel Eu_2TiO_5 ceramics, *J. Am. Ceram. Soc.*, 103 (2020) 4333-4341.
- [6] L. Liu, L. Wang, J. Du, Z. Feng, H. Wu, X. Zhang, P. Gong, Eu_3NbO_7 : Novel middle-dielectric constant microwave dielectric ceramic with monoclinic structure, *Ceram. Int.*, 47 (2021) 13221-13226.
- [7] L.T. Liu, Y.G. Chen, Z.B. Feng, H.T. Wu, X.Y. Zhang, Crystal structure, infrared spectra, and microwave dielectric properties of the EuNbO_4 ceramic, *Ceram. Int.*, 47 (2021) 4321-4326.
- [8] G. Wang, D.N. Zhang, X. Huang, Y.H. Rao, Y. Yang, G.W. Gan, Y.M. Lai, F. Xu, J. Li, Y.L. Liao, C. Liu, L.C. Jin, V.G. Harris, H.W. Zhang, Crystal structure and enhanced microwave dielectric properties of Ta^{5+} substituted $\text{Li}_3\text{Mg}_2\text{NbO}_6$ ceramics, *J. Am. Ceram. Soc.*, 103 (2020) 214-223.
- [9] H.-J. Lee, K.-S. Hong, I.-T. Kim, Crystal structure and microwave dielectric properties of $\text{M}(\text{Nb}_x\text{Ta}_{1-x})_2\text{O}_6$ solid solution ($\text{M}=\text{Mg}$ or Zn), *J. Mater. Res.*, 12 (2011) 1437-1440.
- [10] P. Zhang, Y.G. Zhao, J. Liu, Z.K. Song, X.Y. Wang, M. Xiao, Enhanced microwave dielectric properties of NdNbO_4 ceramic by Ta^{5+} substitution, *J. Alloy. Compd.*, 640 (2015) 90-94.
- [11] Q. Dai, R. Zuo, A novel ultralow-loss Sr_2CeO_4 microwave dielectric ceramic and its property modification, *Journal of the European Ceramic Society*, 39 (2019) 1132-1136.
- [12] S.J. Penn, N.M. Alford, A. Templeton, X.R. Wang, M.S. Xu, M. Reece, K. Schrapel, Effect of porosity and grain size on the microwave dielectric properties of sintered alumina, *J. Am. Ceram. Soc.*, 80 (1997) 1885-1888.
- [13] L. Shi, C. Liu, H. Zhang, R. Peng, G. Wang, X. Shi, X. Wang, W. Wang, Crystal structure, Raman spectroscopy, metal compatibility and microwave dielectric properties of $\text{Ce}_2\text{Zr}_3(\text{MoO}_4)_9$ ceramics, *Mater. Chem. Phys.*, 250 (2020) 7.